

The long-term spin-down trend of ultra-luminous X-ray pulsar M82 X-2

JIREN LIU^{1,2}

¹*Beijing Planetarium, Beijing Academy of Science and Technology, Beijing 100044, China*

²*School of Physical Science and Technology, Southwest Jiaotong University, Chengdu Sichuan 611756, China*

ABSTRACT

The discovery in 2014 of the pulsation from the ultra-luminous X-ray source (ULX) M82 X-2 in 2014 has changed our view of ULXs. Because of the relatively short baseline over which pulsations have been detected so far, M82 X-2's spin state had been assumed to be in an equilibrium state. Using *Chandra* and *XMM-Newton* archive data, we are able to investigate the pulsation of M82 X-2 back to 2005 and 2001. The newly determined spin frequencies clearly show a long-term spin-down trend. If this trend is caused by magnetic threading, we infer a dipolar magnetic field of $\sim 1.2 \times 10^{13}$ G and that a mild beaming factor (~ 4) is needed to match the braking torque with the mass accretion torque. On the other hand, there are *NuSTAR* observations showing instantaneous spin-down behaviours, which might favour a variable prograde/retrograde flow scenario for M82 X-2.

Keywords: Accretion – pulsars: individual: M82 X-2 – X-rays: binaries

1. INTRODUCTION

The discovery of X-ray pulsation from the ultra-luminous X-ray source (ULX) M82 X-2 revealed the existence of accreting magnetized neutron star with an apparent luminosity of around 10^{40} erg s⁻¹ (Bachetti et al. 2014). Since then, a few more ultra-luminous X-ray pulsars (ULXPs) have been identified, e.g., NGC 5907 X-1 (Israel et al. 2017a), NGC 7793 P13 (Fürst et al. 2016; Israel et al. 2017b), NGC 300 X-1 (Carpano et al. 2018), and NGC 1313 X-2 (Sathyaprakash et al. 2019). It is plausible that neutron stars, instead of black holes, are the dominant accretors of the ULX population (for a recent review, see King, Lasota, & Middleton 2023).

Despite being the first discovered ULXP, many properties of M82 X-2 remain unclear. One key property, concerning how the observed luminosity is related to the intrinsic luminosity, is still debated. Mushtukov et al. (2021) showed that a large pulsed fraction ($> 10\%$) implies no strong beaming of ULXPs. Recently, Bachetti et al. (2022) determined an orbital decay rate of -5.69×10^{-8} s s⁻¹ for M82 X-2. This implies a mass transfer rate of ~ 200 times the Eddington limit, which is sufficiently high to produce the observed luminos-

ity and requires no strong beaming. Another unsolved problem concerns the magnetic field of M82 X-2. To reach a luminosity as high as 10^{40} erg s⁻¹, a strong surface magnetic field ($\sim 10^{14}$ G) is needed to reduce the electron scattering opacity. On the other hand, many studies had assumed spin equilibrium of M82 X-2 to estimate its dipolar magnetic field ($\sim 10^{13} - 10^{14}$ G, e.g. Bachetti et al. 2022).

In this paper, we report the detection of pulsation from M82 X-2 back to 2005 (*Chandra* data), and 2001 (*XMM-Newton* data). The subarray mode of *Chandra* ACIS-S has a time resolution of 0.44104s, which makes the detection of a pulse period around 1.35s possible. The *XMM-Newton* EPIC-pn data has a full frame time resolution of 0.07 s, which is also high enough for the detection of pulsation from M82 X-2. The newly measured spin frequencies of M82 X-2 show a surprising long-term spin-down trend, and enable an estimation of the dipolar magnetic field of M82 X-2 based on the braking torque.

2. OBSERVATIONAL DATA

The central region of M82 is very crowd and is generally dominated by M82 X-1 and X-2. Being separated by only $\sim 5''$, currently only *Chandra* can resolve M82 X-2 from M82 X-1. The nominal full frame time of *Chandra* ACIS is 3.2s, too high to detect a pulsation of period around 1.35s. The frame time of the *Chandra* subarray mode is, however, smaller, with 0.44104s for ACIS-S.

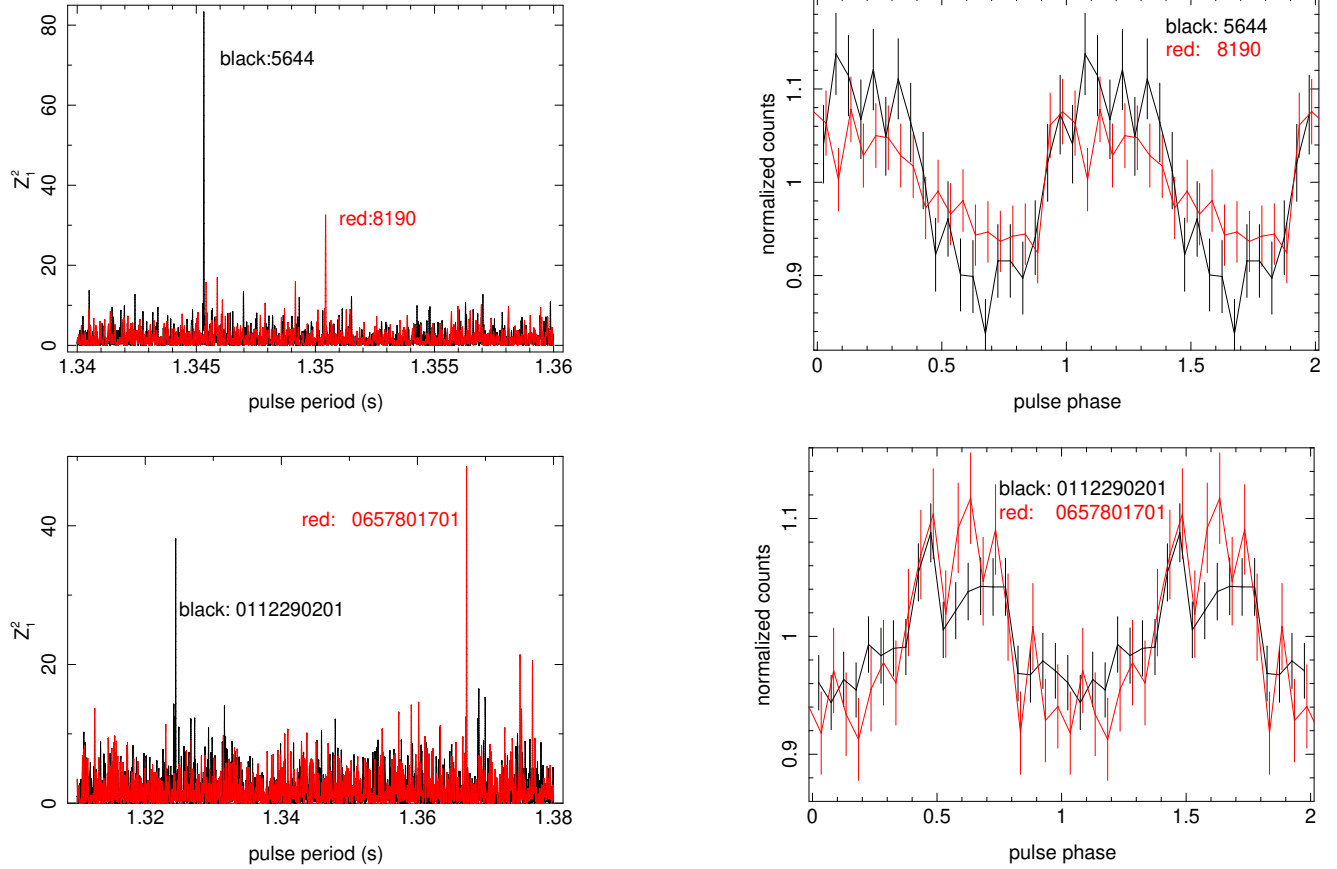


Figure 1. Top: pulsation detection in *Chandra* dataset 5644 and 8190 within 2-8 keV band and their pulse profiles; bottom: pulsation detection in *XMM-Newton* dataset 0112290201 and 0657801701 within 3-8 keV band and their pulse profiles. For viewing purpose, the pulse profiles marked with red are right-shifted a little bit.

This makes *Chandra* subarray data useful for the detection of pulsation from M82 X-2. We searched all the *Chandra* subarray observations of M82, using the standard data products created by the *Chandra* team. The events of M82 X-2 are extracted from a circle region of about $1.7''$ for on-axis observations, and from an ellipse for off-axis observations when the point spread function (PSF) is elongated. The extraction regions were chosen to avoid being blended with nearby sources. The photon count rate is about 0.2 s^{-1} , and we use the events data directly, without rebinning them into a light curve. The background signal is about 5% of that of M82 X-2 and is not taken into account.

XMM-Newton EPIC-pn data have previously been shown to be useful for detecting pulsations from M82 X-2 (Bachetti et al. 2022). To supplement the *Chandra* data, we also searched the *XMM-Newton* EPIC-pn data before 2014. The *XMM-Newton* data were reduced using the *XMM-Newton* science analysis software (SAS, version 20). Circle regions of $30''$ were utilized, and we used the events data. We found two observational episodes showing significant pulsation, which are detailed in Ta-

Table 1. *Chandra* subarray observation and *XMM-Newton* data

Obs.ID	Date	MJD	T_{exp} (ks)	Pulse period ^b (s)	Sig ^c (σ)
0112290201 ^a	2001-05-06	52035	31	1.324474(5)	4.0
6097	2005-02-04	53406	53	-	-
5644	2005-08-17	53599	68	1.345317(2)	7.7
6361	2005-08-18	53600	17	-	-
8190	2007-06-02	54253	53	1.350429(4)	3.3
10027	2008-10-04	54743	18	-	-
0657801701 ^a	2011-04-09	55660	24	1.367224(8)	5.0

^a obsIDs for *XMM-Newton* data;

^b the quoted error is based on Monte-Carlo simulation of the time of arrival of photons from the pulse profile, a method similar as that used in Singhal et al. (2023);

^c the significance of detection in units of σ .

ble 1. All our data were barycentered and corrected for the binary orbital effect using the orbital parameters obtained by Bachetti et al. (2022): $a \sin i = 22.218$ ls, $T_{asc} = 56682.06694$ (MJD), $P_{orb} = 2.5329733$ day, $\dot{P}_{orb} = -5.69 \times 10^{-8} \text{ s s}^{-1}$, and $e = 0$.

3. TIMING RESULTS

We searched all *Chandra* data of M82 with subarray configuration and found 5 observations for which M82 X-2 was bright, as listed in Table 1. We ran the Z_n^2 test (Buccheri et al. 1983) with $n = 1$ to search for pulsation signals over all 5 *Chandra* ACIS subarray datasets. We used the Interactive Spectral Interpretation System (Houck & Denicola 2000), and in particular, the Z_n^2 search routines provided in ISISscripts by the Remeis observatory¹. We searched the period interval between 1.3 s and 1.4 s with a step size of 0.00001 s. We also tried a longer interval and the result is unchanged. We found that the step size needs to be refined to well sample the Z_1^2 peak. The pulsed fraction of M82 X-2 is energy dependent (Bachetti et al. 2022), and becomes smaller at lower energies. We tested different energy ranges for the pulsation signal and found that the 2-8 keV band generally provides the highest statistic. We therefore adopted the energy range of 2-8 keV for our analysis.

The dataset with the longest exposure, 5644, has the highest test value $Z_1^2 = 83$ for the trial period of 1.345317(2) s, as shown in the top left panel of Figure 1. Such a high Z_1^2 value corresponds to a detection significance of about 7.7σ . The uncertainty of the pulsation period is estimated by re-sampling the time of arrival of photons from the folded pulse profile. The Z_1^2 value for dataset 8190 is 33 for a period of 1.350429(4) s, which is also shown in Figure 1. The pulse profiles of both datasets folded with the periods determined are shown in the top right panel of Figure 1, and they are very similar to those reported in Bachetti et al. (2014). To estimate the pulse fraction of a profile, we fitted it with a sinusoidal function with only the fundamental component. The pulse fractions (defined as the semi-amplitude of the sinusoid divided by the mean count rate) are $12 \pm 2\%$ and $6 \pm 2\%$, for dataset 5644 and 8190, respectively. We note that the background is negligible for the on-axis observation 5644, but for the off-axis observation 8190, M82 X-2 is blended with nearby sources (not M82 X-1) and its pulse fraction is only a lower limit. We found no maximum statistics of the other three datasets above 30, and they are neglected hereafter.

For *XMM-Newton* data, the events of M82 X-2 are contaminated with those of M82 X-1, and we found that the energy range of 3-8 keV is more sensitive to the pulsation signal. Searching for the 3-8 keV events, we found two significant Z_1^2 peaks, for observations 0112290201 and 0657801701. The resulting Z_1^2 statistics and pulse profiles are plotted in the bottom panels of Figure 1.

¹ www.sternwarte.uni-erlangen.de/isis

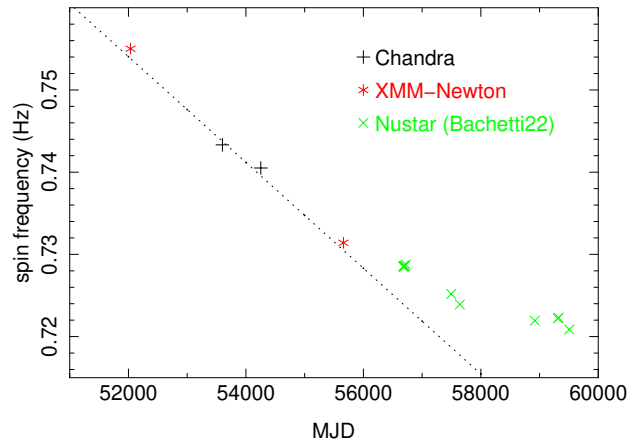


Figure 2. Spin history of M82 X-2 since 2001. The newly measured frequencies clearly indicate a long-term spin-down trend, with a spin-down rate of $-7.4 \times 10^{-11} \text{ Hz s}^{-1}$, which is shown as the dotted line. The uncertainties of the measurements are too small to be illustrated.

The pulse profiles are similar to those of *Chandra* data, with a pulse fraction of $5 \pm 1\%$ and $8 \pm 2\%$, for 0112290201 and 0657801701, respectively. We note that the background level within 3-8 keV of *XMM-Newton* data is around 7%, and the fluxes of M82 X-2 of *XMM-Newton* data include contributions from other sources (not only M82 X-1). These contaminations are hard to estimate without simultaneous *Chandra* observation and may be as luminous as M82 X-2 itself. Therefore, the estimated pulse fraction from *XMM-Newton* data is only a lower limit.

Our newly measured spin frequencies are plotted in Figure 2, together with those measured from *NuSTAR* data by Bachetti et al. (2022). As can be seen, over the 20 years timescale, the spin frequency of M82 X-2 is decreasing continuously. The spin-down rate seems reduced a little around 2021 (MJD 59000), and then returned to its more normal value. The four new detections approximately follow a spin-down rate of $-7.4 \times 10^{-11} \text{ Hz s}^{-1}$, as shown by the dotted line in Figure 2. We note that the four new detections can not be well fitted with a linear function, as the resulting residuals are too large.

The exposure of *Chandra* dataset 5644 is about 70 ks, which is long enough to allow us to constrain the spin frequency derivative ($\dot{\nu}$). We divided the exposure into 2 intervals of 35 ks and measured their pulsations separately. We obtained pulse periods of 1.345321(5) s and 1.345306(4) s around MJD 53599.28 and 53599.71, respectively. These correspond to an averaged spin-up rate of $\sim 2.2 \times 10^{-10} \text{ Hz s}^{-1}$.

4. DISCUSSION AND CONCLUSION

We measured the pulsation of M82 X-2 back to 2005 and 2001 using *Chandra* and *XMM-Newton* archive data. With our newly determined spin frequencies, M82 X-2 shows a clear spin-down trend over a timescale of 20 years, with occasional spin-up events. Such spin behavior is similar to that of Be-type X-ray binaries (BeXBs). BeXBs generally show a spin-up trend during an outburst or giant outburst state, and show a continuous spin-down trend when there is much less mass to be accreted. A typical example is the first Galactic ULXP, Swift J0243.4+6126, which was discovered during a giant outburst in Oct. 2017 (e.g. Wilson-Hodge et al. 2018). After the giant outburst, Swift J0243 showed a continuous spin-down trend (with a rate $\sim -2 \times 10^{-12}$ Hz/s) with its flux being low (Liu et al. 2023).

It is known that M82 X-2 flux shows strong variations and may have a varying period around 60 days (e.g. Brightman et al. 2019). Brightman et al. (2019) found that the overall spectral shape of M82 X-2 is quite similar at low and high levels and the flux variations are unlikely caused by occultations. The changing spin-down/spin-up behavior of M82 X-2 indicates that its accretion torque, and thus its accretion rate, must be varying. Therefore, it is possible that M82 X-2 may have a varying accretion rate, and for long periods of time it is in a relatively quiet state and spins down. A spin-down trend is expected when the accretion rate is low enough that the inner disk radius is larger than the co-rotation radius (R_c), and the magnetic field threading produces a braking torque.

As the ellipticity of M82 X-2 is very small, the origin of the accretion variation of M82 X-2 should be different from the regular type I outbursts from BeXBs. One potential origin of variation is the optical donor star. As recently reported, some classical X-ray pulsars show alternating spin-up/spin-down torque reversals on tens of days (Liao et al. 2022a,b). It was found that for OAO 1657-415 and Vela X-1 their orbital profiles and accretion flows on the orbital scale are different for different torque states, indicating a variation of the flow from the optical donor star over tens of days. Similarly, the accretion flow from M82 X-2's optical star may also vary.

If the long-term spin-down trend of M82 X-2 is caused by magnetic threading, we can infer a dipolar magnetic field based on the magnetic braking torque, as we did for Swift J0243 (Liu et al. 2023). Taking the braking torque as $\tau_b = -\mu^2/9R_c^3$ (Wang et al. 1995; Rappaport et al. 2004) and neglecting the mass accretion torque, we can infer a dipolar magnetic field of $B \sim 1.2 \times 10^{13}$ G, using $2\pi I\dot{\nu} = \tau_b$ and assuming a neutron star of $1.4 M_\odot$ with a radius of 10 km. This dipolar field is similar to that of

Swift J0243 ($B \sim 1.75 \times 10^{13}$ G). While the spin-down rate of M82 X-2 (-7.4×10^{-11} Hz/s) is 35 times higher than that of Swift J0243, its R_c is 3.7 times smaller than that of Swift J0243, which makes the braking torque more efficient.

With the estimated dipolar field of M82 X-2 above, we can compare the braking torque with the accretion torque. During the observation of 5644, the average spin-up rate is about 2.2×10^{-10} Hz/s, which is about twice as high as the average value during the 2014 observations (Bachetti et al. 2014). The unabsorbed 0.5-10 keV luminosity of 5644 is about 1×10^{40} erg/s (Brightman et al. 2016). At such a high luminosity, the accretion disk should be in a radiation pressure dominated state, and the inner disk radius should change very slowly with the accretion rate (Chashkina et al. 2017, 2019):

$$R_{in} \simeq 3.6 \times 10^7 \mu_{30}^{4/9} \sim 8 \times 10^7 \text{ cm}, \quad (1)$$

where μ_{30} is the magnetic moment in units of 10^{30} G cm³. To produce the observed spin-up rate, a mass accretion rate of $\sim 1.3 \times 10^{19}$ g s⁻¹ ($2\pi I\dot{\nu} = \dot{m}\sqrt{GM R_{in}}$) is required, which is about four times less than that inferred from the observed luminosity. That is, a mild beaming factor of about four is needed to match the accretion torque with the braking torque.

However, the long-term spin-down trend of M82 X-2 may be not caused by magnetic threading. Many Galactic X-ray pulsars show alternating spin-up/spin-down reversals, such as OAO 1657-415 (Liao et al. 2022a). The flux of OAO 1657-415 is correlated with the spin-up rate and anti-correlated with the spin-down rate, implying that its torque reversals could be caused by alternating prograde/retrograde accretion flows to the neutron star. A retrograde flow will lead to a spin-down whereas a prograde flow will lead to a spin-up. This implies that the accretion flow (mass transfer) to the neutron star is unstable or variable. One possible scenario is the irradiation-driven instability of a processing warped disk, which may lead to a flip-over inner disk, as first proposed for Cen X-3 by van Kerkwijk et al. (1998).

It is interesting to note that Bachetti et al. (2022) reported some *NuSTAR* observations of instantaneous spin-down behaviors. As *NuSTAR* cannot resolve M82 X-2 from X-1, to make its pulsation detectable by *NuSTAR* data, the fluxes of M82 X-2 would need to be relatively high. In the magnetic braking scenario, to be in a spin-down state, the accretion rate/fluxes should be relatively low. While there were no exact simultaneous *Chandra* data for the *NuSTAR* observations of spin-down, we found that for one *NuSTAR* observation (obsID 30702012002, on MJD 59505, the last data point

in Figure 2), the *Chandra* data observed two days later (obsID 23471) do show a flux ratio between M82 X-2 and X-1 similar to that of data 5644. If confirmed, such spin-down observations of high M82 X-2 fluxes will support a non-magnetic origin for the spin-down of M82 X-2, and a retrograde flow to the neutron star would be preferred. Further monitoring of M82 X-2 with higher cadence using the *Chandra* subarray mode, including both high and low states, is required to reveal the true long-term spin-down nature of M82 X-2.

If the spin-down trend always held in the past, one can infer a spin-down time of $\nu/\dot{\nu} \sim 10^5$ year. Such a time is consistent with the young, star-bursting nature of M82, and may correspond to the formation time of the neutron star of M82 X-2. Nevertheless, we note that spin-up/spin-down reversals on a timescale of years have been observed in X-ray pulsars (such as LMC X-4 [Molkov et al. 2017](#)), and one should be cautious when inferring a longer-term trend.

ACKNOWLEDGEMENTS

We thank the referee for his/her thoughtful comments which have improved the paper considerably and Richard Long for a through reading. This work used data from *XMM-Newton* telescope and employed a list of *Chandra* datasets, obtained by the *Chandra* X-ray Observatory, contained in DOI: [cdc.172](#). This research has made use of a collection of ISIS functions (ISISscripts) provided by ECAP/Remeis observatory and MIT (<http://www.sternwarte.uni-erlangen.de/isis/>). We acknowledge the support by National Natural Science Foundation of China (U1938113), the Scholar Program of Beijing Academy of Science and Technology (DZ BS202002), and the science research grants from the China Manned Space Project.

REFERENCES

- Bachetti, M.; Harrison, F. A.; Walton, D. J. et al. 2014, *Nature*, 514, 202
- Bachetti, M.; Heida, M.; Maccarone, T. et al. 2022, *ApJ*, 937, 125
- Brightman, M.; Harrison, F. A.; Walton, D. J.; Fürst, F. et al. 2016, *ApJ*, 816, 60
- Brightman, M.; Harrison, F. A.; Bachetti, M.; Xu, Y.; Fürst, F.; Walton, D. J.; Ptak, A. et al. 2019, *ApJ*, 873, 115
- Buccheri, R.; Bennett, K.; Bignami, G. F.; Bloemen, J. B. G. M.; Boriakoff, V.; Caraveo, P. A.; Hermsen, W.; Kanbach, G. et al. 1983, *A&A*, 128, 245
- Carpano, S.; Haberl, F.; Maitra, C.; Vasilopoulos, G., 2018, *MNRAS*, 476, L45
- Chashkina, A.; Abolmasov, P.; Poutanen, J. 2017, *MNRAS*, 470, 2799
- Chashkina, A.; Lipunova, G.; Abolmasov, P.; Poutanen, J. 2019, *A&A*, 626, 18
- Fürst, F.; Walton, D. J.; Harrison, F. A. et al. 2016, *ApJ*, 831, L14
- Houck, J. C. & Denicola, L. A. 2000, *ASPC*, 216, 591
- Israel, G. L.; Belfiore, A.; Stella, L. et al., 2017, *Sci*, 355, 817
- Israel, G. L.; Papitto, A.; Esposito, P. et al., 2017, *MNRAS*, 466, L48
- King, A., Lasota, J. & Middleton, M. 2023, *NewAR*, 9601672
- Liao, Z.; Liu, J.; Jenke, P. A.; Gou, L. 2022, *MNRAS*, 510, 1765
- Liao, Z.; Liu, J.; Gou, L. 2022, *MNRAS*, 517L, 111
- Liu, J.; Ji, L.; Ge, M. 2023, *ApJ*, 950, 42
- Molkov, S.; Lutovinov, A.; Falanga, M.; Tsygankov, S.; Bozzo, E., C. 2017, *MNRAS*, 464, 2039
- Mushtukov, A. A.; Portegies Zwart, S.; Tsygankov, S. S.; Nagirner, D. I.; Poutanen, J. 2021, *MNRAS*, 501, 2424
- Rappaport, S. A.; Fregeau, J. M.; Spruit, H. 2004, *ApJ*, 606, 436
- Sathyaprakash, R.; Roberts, T. P.; Walton, D. J. et al. 2019, *MNRASL*, 488, 35
- Singhal, A.; Jain, I.; Bala, S; Bhalerao, V. 2023, [arxiv:231106620](#)
- van Kerkwijk M. H., Chakrabarty D., Pringle J. E., Wijers R. A. M. J., 1998, *ApJ*, 499, L27
- Wang, Y. M. 1995, *ApJ*, 449, L153
- Wilson-Hodge, C. A.; Malacaria, C.; Jenke, P. A. et al. 2018, *ApJ*, 863, 9